Karenwebberite, Na(Fe^{2+},Mn^{2+})PO$_4$, a new member of the triphylite group from the Malpensata pegmatite, Lecco Province, Italy

PIETRO VIGNOLA,[1] FRÉDÉRIC HATERT,[2,*] ANDRÉ-MATHIEU FRANSOLET,[2] OLAF MEDENBACH,[3] VALERIA DIELLA,[1] AND SERGIO ANDÒ[4]

[1]CNR-Istituto per la dinamica dei processi ambientali, via Mario Bianco, 9-20131 Milao, Italy
[2]Laboratoire de Minéralogie, Département de Géologie, Université de Liège, Bâtiment B18, Sart Tilman, B-4000 Liège, Belgium
[3]Institut für Geologie, Mineralogie une Geophysik, Ruhr-Universität Bochum, Universitätsstrasse 150, D-44780 Bochum, Germany
[4]Dipartimento di Scienze Geologiche e Geotecnologie, Università di Milano-Bicocca-piazzale della Scienza 4, 20126 Milano, Italy

ABSTRACT

Karenwebberite, Na(Fe^{2+},Mn^{2+})PO$_4$, belongs to the triphylite group of minerals and corresponds to the Fe-equivalent of natrophilite or to the Na-equivalent of triphylite. It occurs in the Malpensata pegmatite dike, Colico, Lecco Province, Italy. Karenwebberite is found as late-magmatic-stage exsolution lamellae up to 100 μm thick, hosted by graftonite and associated with Na-bearing ferrisicklerite and with a heterosite-like phase. Lamellae are pale green, with very pale grayish-green streak. The luster is greasy to vitreous, and lamellae are translucent (pale green) to opaque (dark green). Optically, the mineral is anisotropic, biaxial (+), α = 1.701(2), β = 1.708(2), γ = 1.717(2) (for λ = 589 nm), $2V_{meas}$ = 87(4)°, $2V_{calc}$ = 41°, Z = b. Pleochroism is moderate with X = dark gray, Y = brown, and Z = yellow. The mineral is brittle with a Mohs hardness of 4.5; in thin section it displays a perfect cleavage along {001} with an irregular fracture. Karenwebberite is non-fluorescent either under short-wave or long-wave ultraviolet light, and its calculated density is 3.65 g/cm^3. The mean chemical composition, determined by the electron microprobe from 16 point analyses (wt%), is: P$_2$O$_5$ 41.12, Fe$_2$O$_3$* 7.00, FeO* 25.82, MgO 0.23, ZnO 0.11, MnO 9.31, CaO 0.10, Na$_2$O 14.66, total 98.41 (*: calculated values). The empirical formula, calculated on the basis of 1 P atom per formula unit from, is (Na$_{0.817}$Ca$_{0.003}$□$_{0.180}$)$_{\Sigma1.000}$ (Fe$^{2+}_{0.622}$Mn$^{2+}_{0.228}$Fe$^{3+}_{0.151}$Mg$_{0.010}$Zn$_{0.002}$)$_{\Sigma1.013}$PO$_4$. Karenwebberite is orthorhombic, space group *Pbnm*, a = 4.882(1), b = 10.387(2), c = 6.091(1) Å, V = 308.9(1) Å^3, and Z = 4. The mineral possesses the olivine structure, with the M1 octahedra occupied by Na, and the M2 octahedra occupied by Fe and Mn. The eight strongest lines in the X-ray powder pattern are [d in Å (intensities) (hkl)]: 5.16 (50) (020), 4.44 (90) (110), 3.93 (80) (021), 3.56 (90) (120), 3.04 (80) (002), 2.817 (100) (130), 2.559 (100) (131), and 1.657 (50) (061). The mineral is named in honor of Karen Louise Webber, Assistant Professor Research at the Mineralogy, Petrology and Pegmatology Research Group, Department of Earth and Environmental Sciences, University of New Orleans, Louisiana, U.S.A.

Keywords: Karenwebberite, new mineral, phosphate, Malpensata pegmatite, Lecco Province, Italy, pegmatites

INTRODUCTION

The triphylite mineral group is constituted by several Fe-Mn-bearing phosphates, which are widespread in medium to highly evolved LCT granitic pegmatites, ranging from the beryl-columbite-phosphate subtype to the spodumene subtype, according to the classification of Černý and Ercit (2005). This group contains primary and weakly oxidized phosphates, as for example minerals of the triphylite-lithiophilite solid-solution series [Li(Fe^{2+},Mn)PO$_4$–Li(Mn,Fe^{2+})PO$_4$] and natrophilite [Na(Mn,Fe^{2+})PO$_4$], but the oxidation also frequently produces more oxidized phosphates as ferrisicklerite-sicklerite [□$_{1-x}$Li$_x$(Fe^{3+},Mn^{2+})PO$_4$–□$_{1-x}$Li$_x$(Mn^{2+},Fe^{3+})PO$_4$] or heterosite-purpurite [□(Fe^{3+},Mn^{3+})PO$_4$–□(Mn^{3+},Fe^{3+})PO$_4$].

Triphylite hosted by Triassic pegmatites embedded into the crystalline basement of the central Southern Alps had been recently described at Brissago (Switzerland) and Piona (Italy) (Vignola et al. 2008a, 2010, 2011a). In this paper, we report the description of a new Na-bearing mineral species belonging to the triphylite group, karenwebberite, Na(Fe^{2+},Mn^{2+})PO$_4$ (IMA 2011-015, Vignola et al. 2011b).

The mineral was found by one of the authors (P.V.) at the Malpensata granitic pegmatite, Colico commune, Lecco Province, north Italy. The Malpensata dike, mined for ceramic feldspar and mica during 1943–1946, is located on the east side of the Piona peninsula, 1.2 km north of Olgiasca village and 200 m south of the Piona Abbey, at an elevation of 110 m above sea level (46°, 07′, 20″N; 9°, 10′, 33″E). The Malpensata dike belongs to the Piona granitic pegmatite swarm, which is embedded into the high-grade metapelites (sillimanite-, biotite-bearing micaschists

and gneisses) of the Dervio-Olgiasca Zone that constitutes the crystalline basement of the Central Southern Alps (Bertotti et al. 1999). The dike consists of plagioclase (An_{08}) and quartz, with muscovite, schorl, and almandine-rich garnet as common accessories, and belongs to the beryl-columbite-phosphate sub-type of LCT granitic pegmatites referred to the classification of P. Černý (Černý and Ercit 2005; Vignola et al. 2010). Karenwebberite occurs as thin exsolution lamellae within graftonite nodules, which are enclosed in blocky plagioclase crystals located in the central portion (the most evolved one) of the dike. These nodules were found in close association with cassiterite, Hf-rich zircon, tapiolite-(Fe), oxycalciomicrolite, ferrowyllieite, and other evolved phosphates (Vignola et al. 2008b, 2010).

The mineral has been approved by the Commission on New Minerals and Mineral Names of the International Mineralogical Association under number IMA 2011-015, and is named in honor of Karen Louise Webber, who is Assistant Professor Research at the Mineralogy, Petrology, and Pegmatology Research Group, Department of Earth and Environmental Sciences, University of New Orleans, Louisiana, U.S.A. Her research has focused on the cooling and crystallization dynamics of granitic pegmatites; in particular, she has demonstrated that crystal size is not a reliable indicator of crystallization time in pegmatites. For the analyses described in the following sections, two co-type specimens originating from the same hand sample were used. The two co-type specimens are kept in the mineralogical collection of the Museum of Natural History of Milano (Italy), catalog number M37902 and in the mineralogical collection of the Department of Geology of the University of Liège (Belgium), catalog number 20385.

APPEARANCE AND PHYSICAL PROPERTIES

Karenwebberite forms pale to dark green (brownish if oxidized), transparent to translucent, exsolution lamellae up to 50–80 μm thick and 2–4 mm long, included in very pale-pink graftonite. Figure 1 shows karenwebberite in thin section. Due to iron oxidation, this mineral progressively transforms into Na-bearing ferrisicklerite, $Na_{1-x}(Fe^{3+},Mn^{2+})PO_4$, which shows a dark brown color in thin section (Fig. 1). Lamellae of karenwebberite display a perfect cleavage along the {001} direction, as observed in thin section. The mineral is brittle and the Mohs hardness is 4.5(5), estimated by comparison with other minerals of the triphylite group. The luster is greasy to vitreous and the streak is very pale grayish green. Karenwebberite is biaxial (+), $\alpha = 1.701(2)$, $\beta = 1.708(2)$, $\gamma = 1.717(2)$ (for $\lambda = 589$ nm), $2V_{meas} = 87(4)°$, $2V_{calc} = 41°$, with $Z \| b$. Pleochroism is moderate with X = dark gray, Y = brown, and Z = yellow. Karenwebberite is non-fluorescent either under short-wave (254 nm) or long-wave (366 nm) ultraviolet light. Due to the small grain size, the density was not measured directly, but the density calculated from the empirical formula and single-crystal data is 3.65 g/cm³. The compatibility index (Mandarino 1981), based upon the empirical formula, calculated density, and average index of refraction, is $1 - (Kp/Kc) = 0.010$, which corresponds to the superior category.

CHEMICAL COMPOSITION

Preliminary chemical investigations of karenwebberite were performed on a polished thin section using a Tescan Vega TS 5136 XM scanning electron microscope (SEM) equipped with an
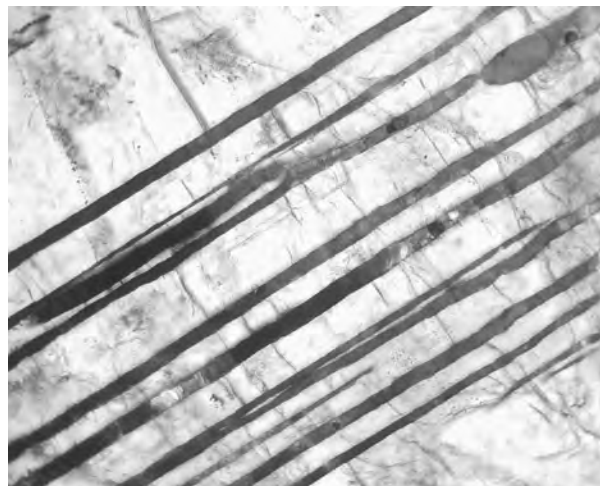

FIGURE 1. Exsolution lamellae of karenwebberite (light brown), oxidized into Na-bearing ferrisicklerite (dark brown) and included in graftonite. Malpensata pegmatite, Colico, Italy (plane-polarized light microscopy; the length of the photograph is 1.5 mm).

EDAX Genesis 4000 JXM energy-dispersive spectrometer (EDS) at the "Centro interdipartimentale di microscopia elettronica" of the University of Milano-Bicocca.

Quantitative chemical analyses were performed on the same polished thin section using a JEOL JXA-8200 electron microprobe operating in wavelength-dispersive mode at the laboratory of the Department of Earth Sciences, University of Milano. The accelerating voltage was 15 kV, with a beam current of 15 nA, a spot size of 2 μm, and a counting time of 30 s on the peaks and 10 s on the background. Natural minerals were used as standards (graftonite KF16 for P, Fe, Mn and Ca; olivine USNM 2566 for Mg; rhodonite for Zn; and omphacite USNM 110607 for Na). The raw data were corrected for matrix effects using the ΦρZ method from the JEOL series of programs. The mean analytical results (average of 16 point analyses) are reported in Table 1. H_2O and CO_2 were not determined directly because of the small amount of material; anyway, these groups are absent from the mineral, as shown by the structural results (see below). The empirical formula, calculated on the basis of 1 P atom per formula unit with the $Fe^{2+}:Fe^{3+}$ ratio constrained to maintain charge balance, is

$$(Na_{0.817}Ca_{0.003}\square_{0.180})_{\Sigma1.000}(Fe^{2+}_{0.622}Mn^{2+}_{0.228}Fe^{3+}_{0.151}Mg_{0.010}Zn_{0.002})_{\Sigma1.013}PO_4$$

TABLE 1. Averaged electron-microprobe analyses of karenwebberite

	wt% (average of 16 analyses)	Range	St. dev.	Empirical formula†	
P_2O_5	41.12	40.21–42.53	0.71	P (apfu)	1.000
Fe_2O_3*	7.00	–	–	Fe^{3+}	0.151
FeO*	25.82	24.89–27.10	0.67	Fe^{2+}	0.622
MgO	0.23	0.21–0.27	0.02	Mg	0.010
ZnO	0.11	0.04–0.19	0.04	Zn	0.002
MnO	9.31	8.92–9.54	0.21	Mn	0.228
CaO	0.10	0.05–0.20	0.04	Ca	0.003
Na_2O	14.66	13.95–16.12	0.63	Na	0.817
Total	98.35				

* FeO and Fe_2O_3 contents were calculated to maintain charge balance.
† Calculated on the basis of 1 P atom per formula unit (apfu).

The simplified formula is $Na(Fe^{2+},Mn^{2+})PO_4$, which requires Na_2O 17.86 wt%, FeO 27.74 wt%, MnO 13.49 wt%, P_2O_5 40.91 wt%, for a Fe:Mn ratio of 0.67:0.33 (based on refined site occupancies), reaching a total of 100.00 wt%.

X-RAY DIFFRACTION DATA AND CRYSTAL STRUCTURE DETERMINATION

Karenwebberite was first identified by powder X-ray diffraction using a Debye-Scherrer camera (diameter 114.6 mm, FeKα radiation); the unit-cell parameters refined from the powder XRD pattern (Table 2) using the LCLSQ software (Burnham 1991) are: $a = 4.91(1)$, $b = 10.33(6)$, $c = 6.09(2)$ Å, and $V = 309(3)$ Å^3 ($Z = 4$, space group $Pbnm$).

The X-ray structural study of karenwebberite was carried out on an Oxford Diffraction Gemini PX Ultra 4-circle diffractometer equipped with a Ruby CCD-area detector (FUNDP, Namur, Belgium), on a crystal fragment measuring $0.04 \times 0.09 \times 0.13$ mm. A total of 130 frames with a spatial resolution of 1° were collected by the φ/ω scan technique, with a counting time of 55 s per frame, in the range $7.84° < 2\theta < 58.16°$. A total of 861 re-flections were extracted from these frames, corresponding to 397 unique reflections. The unit-cell parameters refined from these reflections, $a = 4.882(1)$, $b = 10.387(2)$, $c = 6.091(1)$ Å, and $V = 308.9(1)$ Å^3, are in good agreement with those refined from the X-ray powder diffraction data. Data were corrected for Lorentz, polarization and absorption effects, the latter with an empirical method using the SCALE3 ABSPACK scaling algorithm included in the CrysAlisRED package (Oxford Diffraction 2007).

The crystal structure of karenwebberite was refined with SHELXTL (Sheldrick 2008) in space group $Pbnm$, starting from the atomic coordinates used by Losey et al. (2004) for triphylite. Scattering curves for neutral atoms, together with anomalous dispersion corrections, were taken from the *International Tables for X-ray Crystallography*, vol. C (Wilson 1992). For the sake of simplicity, Mg, Zn, and Ca, which occur in low to trace amounts, were not taken into account in the crystal structure refinements. Finally, the relative occupancies of Na and vacancies on M1, as well as of Fe and Mn on M2, were refined. The refinements were completed using anisotropic displacement parameters for all atoms. The final refinement converged to $R_1 = 0.0785$ [$F_o > 2\sigma(F_o)$] for 375 reflections and $R_1 = 0.0835$ for all 397 reflections. Further details on the intensity data collection and structure refinement are given in Table 3. (CIF available on deposit.[1])

TABLE 2. X-ray powder diffraction pattern of karenwebberite

I_{obs}	d_{obs}	I_{calc}	d_{calc}	hkl
50	**5.16**	**25**	**5.164**	**0 2 0**
90	**4.44**	**48**	**4.435**	**1 1 0**
80	**3.93**	**37**	**3.939**	**0 2 1**
20	3.79	8	3.823	1 0 1
90	**3.56**	**86**	**3.559**	**1 2 0**
80	**3.04**	**52**	**3.046**	**0 0 2**
100	**2.817**	**57**	**2.819**	**1 3 0**
100	**2.559**	**100**	**2.558**	**1 3 1**
30	2.386	25	2.389	2 1 0
40	2.302	15	2.314	1 2 2
		13	2.285	1 4 0
30	2.219	13	2.218	2 2 0
40	1.921	1	1.912	2 0 2
20	1.789	46	1.793	2 2 2
30	1.709	20	1.708	2 4 1
50	**1.657**	**25**	**1.656**	**0 6 1**
20	1.604	6	1.615	1 5 2
		15	1.596	0 4 3

Notes: Intensities were estimated visually. The eight strongest lines are in bold. Calculated intensities were calculated from the structural data with the SHELX-TL-XPOW software (Sheldrick 1990). Uncertainties are ca. 1% of the d_{obs} values.

TABLE 3. Experimental details for the single-crystal X-ray diffraction study of karenwebberite

|	
Color	Pale green
Dimensions of the crystal (mm)	ca. $0.04 \times 0.09 \times 0.13$
a (Å)	4.882(1)
b (Å)	10.387(2)
c (Å)	6.091(1)
V (Å^3)	308.9(1)
Space group	$Pbnm$
Z	4
$2\theta_{min}, 2\theta_{max}$	7.84°, 58.16°
Range of indices	$-6 \leq h \leq 4$, $-9 \leq k \leq 13$, $-8 \leq l \leq 5$
Measured intensities	861
Unique reflections	397
Independent non-zero [$I > 2\sigma(I)$] reflections	375
μ (mm^{-1})	5.217
Refined parameters	43
R_1 [$F_o > 2\sigma(F_o)$]	0.0785
R_1 (all)	0.0835
wR_2 (all)	0.2055
S (goodness of fit)	1.269
Max Δ/σ in the last l.s. cycle	0.001
Max peak and hole in the final ΔF map (e/Å^3)	+1.12 and −2.20
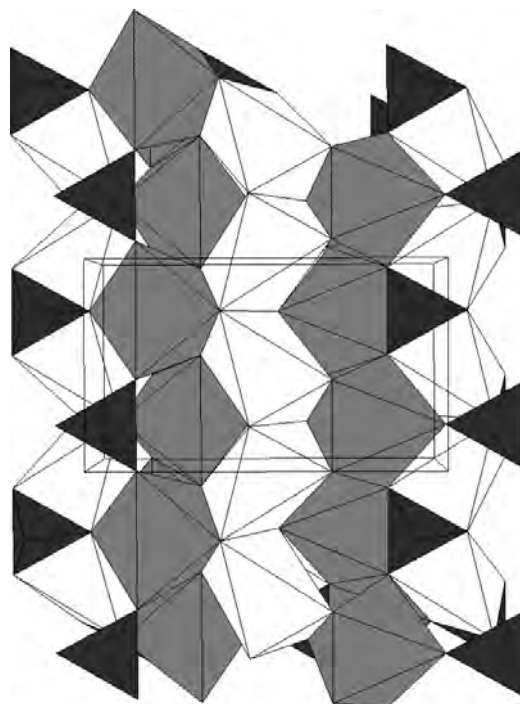
FIGURE 2. The crystal structure of karenwebberite, projected along the **a** axis. The M1 octahedra are white, the M2 octahedra are light gray, and the PO$_4$ tetrahedra are dark gray.

TABLE 4. Final fractional coordinates and displacement parameters (Å²) for karenwebberite

Site	x	y	z	U_{eq}	U_{11}	U_{22}	U_{33}	U_{23}	U_{13}	U_{12}
M1*	0	0	0	0.018(3)	0.008(4)	0.025(5)	0.021(5)	–0.003(4)	–0.007(3)	0.002(3)
M2†	0.9862(4)	0.2827(2)	¼	0.0103(7)	0.017(1)	0.010(1)	0.005(1)	0	0	–0.0008(7)
P	0.4334(8)	0.1034(4)	¼	0.0122(9)	0.017(2)	0.013(2)	0.007(2)	0	0	0.002(1)
O1	0.744(2)	0.111(1)	¼	0.019(2)	0.019(5)	0.024(6)	0.015(5)	0	0	0.006(5)
O2	0.166(3)	0.4648(9)	¼	0.020(2)	0.037(7)	0.010(5)	0.013(5)	0	0	–0.011(5)
O3	0.303(2)	0.1737(7)	0.052(1)	0.019(2)	0.026(4)	0.025(4)	0.005(3)	0.008(3)	0.000(3)	0.006(3)

Note: Occupancy factors: * 0.68(3) Na; † 0.67(8) Fe + 0.33(8) Mn.

TABLE 5. Selected bond distances (Å) and angles (°) for karenwebberite

M1-O1 x2	2.284(8)
M1-O2 x2	2.261(9)
M1-O3 x2	2.354(8)
Mean	2.300
M2-O1	2.14(1)
M2-O2	2.09(1)
M2-O3 x2	2.092(7)
M2-O3' x2	2.266(8)
Mean	2.158
P-O1	1.52(1)
P-O2	1.52(1)
P-O3 x2	1.550(7)
Mean	1.535
O1-P-O2	111.7(7)
O1-P-O3 x2	112.6(4)
O2-P-O3 x2	108.4(4)
O3-P-O3	102.6(6)
Mean	109.38

Karenwebberite possesses the olivine structure and is isostructural with the pegmatite phosphates triphylite, lithiophilite, and natrophilite (Finger and Rapp 1969; Moore 1972; Losey et al. 2004; Fehr et al. 2007). The structure is characterized by octahedral chains parallel to the **c** axis (Fig. 2). The M1 octahedra are occupied by Na, while the M2 octahedra are occupied by Fe and Mn (Table 4). Bond distances and the most relevant bond angles are summarized in Table 5. It is noteworthy that this ordered distribution, with Na localized on the M1 site, is similar to the cationic distribution observed by Moore (1972) in natrophilite. The crystal-chemical formula of karenwebberite, calculated from the site occupancy factors (Table 4), is $Na_{0.68}(Fe^{2+}_{0.67}Mn_{0.33})PO_4$, and corresponds fairly well to the empirical formula calculated from the electron microprobe analyses.

DISCUSSION

Karenwebberite is isostructural with olivine and corresponds to the Fe-analog of natrophilite, $NaMnPO_4$, or to the Na-equivalent of triphylite, $LiFePO_4$. The mineral is also a polymorph of maricíte, $NaFePO_4$ [$a = 6.861(1)$, $b = 8.987(1)$, $c = 5.045(1)$ Å, $Pmnb$], which shows a crystal structure distinct from that of olivine (Sturman et al. 1977; Le Page and Donnay 1977). A comparison of the physical properties of karenwebberite, with those of phosphates of the triphylite group, is shown in Table 6.

The polymorphic relationship between karenwebberite and maricíte is also of particular interest, since this transformation is temperature-dependent, as shown experimentally by Corlett and Armbruster (1979). These authors confirmed that olivine-type $Na(Fe,Mn)PO_4$ phosphates are low-temperature polymorphs of maricíte-type phosphates, and that the transition between the

TABLE 6. Comparison of the physical properties for phosphates of the triphylite group

Mineral	Triphylite	Lithiophilite	Natrophilite	Karenwebberite
Reference	[1, 2]	[1, 2]	[3, 4]	This work
Ideal formula	$Li(Fe^{2+},Mn^{2+})PO_4$	$Li(Mn^{2+},Fe^{2+})PO_4$	$Na(Mn^{2+},Fe^{2+})PO_4$	$Na(Fe^{2+},Mn^{2+})PO_4$
Space group	$Pbnm$	$Pbnm$	$Pbnm$	$Pbnm$
a (Å)	4.6904(6)	4.7383(1)	4.987(2)	4.882(1)
b (Å)	10.2855(9)	10.429(1)	10.523(5)	10.387(2)
c (Å)	5.9871(4)	6.0923(4)	6.312(3)	6.091(1)
Z	4	4	4	4
Strong X-ray lines	5.175 (34)	5.236 (28)	5.24 (30)	5.16 (25)
	4.277 (76)	4.313 (56)	4.50 (60)	4.44 (48)
	–	–	4.05 (60)	–
	3.923 (26)	–	3.90 (30)	3.93 (37)
	–	–	3.66 (50)	3.79 (8)
	3.487 (70)	3.516 (71)	3.61 (10)	3.56 (86)
	3.008 (100)	3.051 (89)	3.15 (50)	3.04 (52)
	–	–	2.863 (80)	–
	2.781 (34)	–	–	2.817 (57)
	–	–	2.702 (20)	–
	–	–	2.604 (100)	–
	2.525 (81)	2.548 (100)	2.583 (100)	2.559 (100)
	–	2.492 (28)	2.487 (30)	–
Cleavage	{001} perfect, {010} imperfect	{001} perfect, {010} good	{001} good, {010} indistinct, {120} interrupted	{001} perfect
Density	3.54(4)	3.47(3)	3.41; 3.47 (calc.)	3.65 (calc.)
Optical sign	(+)	(+)	(+)	(+)
2V (°)	0–55	48–70	75(5)	87(4)
α	1.675–1.694	1.663–1.696	1.671(3)	1.701(2)
β	1.684–1.695	1.667–1.700	1.674(3)	1.708(2)
γ	1.685–1.700	1.674–1.702	1.684(3)	1.717(2)
Hardness	4–5	4–5	4.5–5	4.5(5)
Color	Bluish grey to greenish grey	Yellowish brown, honey-yellow, grey	Deep wine-yellow	Pale green; brownish when oxidized

Notes: [1] Losey et al. (2004), [2] Anthony et al. (1990), [3] Moore (1972), [4] Palache et al. (1951).
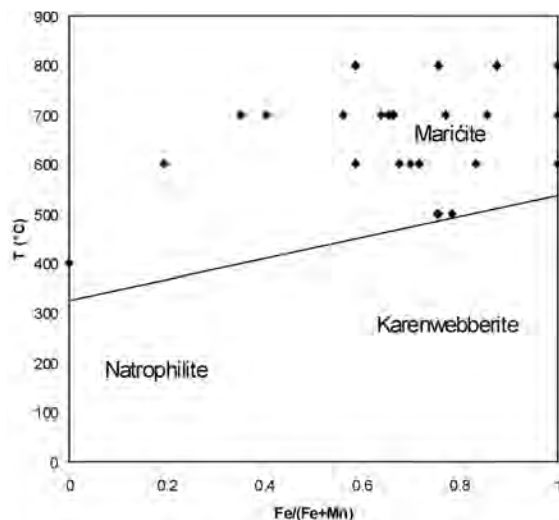
FIGURE 3. Stability of natrophilite, karenwebberite and marićite in the Fe/(Fe+Mn) – T field. The points represent the chemical compositions of synthetic marićites reported by Hatert et al. (2006, 2011), and the high-temperature stability limit of natrophilite has been constrained from the data published by Corlett and Armbruster (1979).

FIGURE 4. Ternary Na-Fe_{tot}-Mn_{tot} plot showing the electron microprobe analyses of karenwebberite (black dots), Na-bearing ferrisicklerite (squares), and the heterosite-like phase (diamonds). The percentages correspond to atomic proportions.

TABLE 7. Electron microprobe analyses of Na-bearing ferrisicklerite and heterosite-like phase

	a (2)	b (6)	c (2)	d (3)
P_2O_5	42.96	43.72	44.11	46.58
Fe_2O_3*	12.71	21.14	24.44	40.06
Mn_2O_3*	–	–	–	6.06
FeO*	22.16	15.46	13.43	–
MgO	0.25	0.27	0.26	0.27
ZnO	0.10	0.17	0.10	0.13
MnO*	10.07	9.88	10.03	5.18
CaO	0.09	0.09	0.10	0.08
Na_2O	13.00	10.03	8.39	2.10
Total	101.34	100.76	100.86	100.46
Cation number on the basis of 1 P atom per formula unit				
P	1.000	1.000	1.000	1.000
Fe^{3+}	0.263	0.430	0.492	0.764
Mn^{3+}	–	–	–	0.117
Fe^{2+}	0.510	0.349	0.301	–
Mg	0.010	0.011	0.010	0.010
Zn	0.002	0.003	0.002	0.002
Mn^{2+}	0.234	0.226	0.227	0.111
Ca	0.003	0.003	0.003	0.002
Na	0.694	0.526	0.436	0.103
ΣM2	1.019	1.019	1.032	1.004
ΣM1	0.697	0.529	0.439	0.105

Notes: Analyses in weight percents; the number of point analyses is indicated in parentheses. a = Na-rich ferrisicklerite; b = Intermediate ferrisicklerite; c = Na-poor ferrisicklerite; d = Heterosite-like phase. Uncertainties are ca. 5% of the wt% values.
* FeO, Fe_2O_3, MnO, and Mn_2O_3 contents were calculated to maintain charge balance.

two polymorphs of $NaMnPO_4$ occurs around 325 °C ($P = 100$ bars). Hydrothermal investigations performed on alluaudite-type phosphates at 1 kbar (Hatert et al. 2006, 2011) also produced several marićite-type phosphates with various Fe/(Fe+Mn) ratios; their compositions are plotted in Figure 3. From this diagram, on which the transition temperature from natrophilite to its polymorph has been constrained according to the data of Cor-
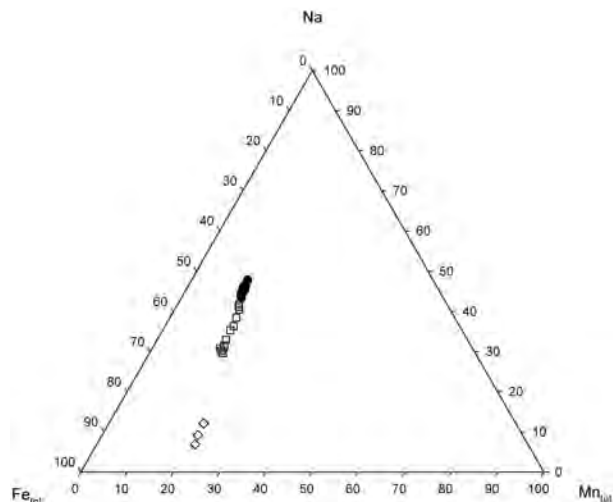
lett and Armbruster (1979), we can clearly observe a transition temperature of about 500–550 °C between karenwebberite and marićite. Consequently, karenwebberite certainly crystallized below 550 °C in the Malpensata dike.

During the evolution of the oxidation condition in this pegmatite, karenwebberite progressively oxidized into a reddish-brown phosphate, as shown on the thin sections (Fig. 1). This phosphate shows a chemical composition significantly depleted in Na, compared to karenwebberite, and both phosphates are isostructural, as confirmed by single-crystal X-ray diffraction measurements. This secondary phosphate corresponds to a Na-bearing ferrisicklerite, according to its optical and structural properties, and its chemical composition evolves from $(Na_{0.69}\square_{0.31})(Fe^{2+}_{0.51}Fe^{3+}_{0.26}Mn^{2+}_{0.23}Mg_{0.01})$ PO_4 to $(Na_{0.44}\square_{0.56})(Fe^{3+}_{0.49}Fe^{2+}_{0.30}Mn^{2+}_{0.23}Mg_{0.01})PO_4$ (Table 7). This oxidation mechanism, from karenwebberite to Na-bearing ferrisicklerite, is similar to that observed during the concomitant leaching of Li^+ and oxidation of Fe^{2+} in triphylite, leading to ferrisicklerite. It certainly took place during the late hydrothermal stages affecting the pegmatite, and corresponds to the substitution mechanism $Na^+ + Fe^{2+} \rightarrow \square + Fe^{3+}$, previously reported in alluaudite- and wyllieite-type phosphates by Quensel (1957), Fransolet et al. (1985, 2004), and Roda et al. (1996).

Figure 4 plots the chemical analyses of the oxidation products of karenwebberite, and shows a continuous depletion of Na from karenwebberite to Na-poor ferrisicklerite, with a constant Fe/(Fe+Mn) ratio. However, a lack of data is observed between ca. 0.44 and 0.14 Na apfu, which can tentatively be related to the transformation of Na-poor ferrisicklerite to a heterosite-like phase. Indeed, as shown on Table 7, a progressive oxidation of Fe^{2+} to Fe^{3+} is observed for Na-bearing ferrisicklerite, whereas all iron and ca. 51% of manganese are oxidized in the heterosite-like phase. This gap in data could have resulted from the sudden oxidation of manganese in these olivine-type phosphates.

REFERENCES CITED

Anthony, J.W., Bideaux, R.A., Bladh, K.W., and Nichols, M.C. (1990) Handbook of mineralogy. Mineral Data Publishing, Tucson, Arizona, U.S.A.

Bertotti, G., Seward, D., Wijbrans, J., ter Voorde, M., and Hurford, A.J. (1999) Crustal thermal regime prior to, during, and after rifting: A geochronological and modeling study of the Mesozoic South Alpine rifted margin. Tectonics, 18/2, 185–200.

Burnham, C.W. (1991) LCLSQ version 8.4, least-squares refinement of crystallographic lattice parameters. Department of Earth and Planetary Sciences, Harvard University, 24 p.

Černý, P. and Ercit, S. (2005) The classification of granitic pegmatites revisited. Canadian Mineralogist, 43, 2005–2026.

Corlett, M.I. and Armbruster, T. (1979) Structural relations between maricíte and natrophilite in the system NaFePO4-NaMnPO4. GAC-MAC Join annual meeting, 4, 1979.

Fehr, K.T., Hochleitner, R., Schmidbauer, E., and Schneider, J. (2007) Mineralogy, Mössbauer spectra and electrical conductivity of triphylite, $Li(Fe^{2+},Mn^{2+})PO_4$. Physics and Chemistry of Minerals, 34, 485–494.

Finger, L.W. and Rapp, G.R. (1969) Refinement of the structure of triphylite. Carnegie Institution Yearbook, 68, 290–293.

Fransolet, A.-M., Abraham, K., and Speetjens, J.-M. (1985) Evolution génétique et signification des associations de phosphates de la pegmatite d'Angarf-Sud, plaine de Tazenakht, Anti-Atlas, Maroc. Bulletin de Minéralogie, 108, 551–574.

Fransolet, A.-M., Hatert, F., and Fontan, F. (2004) Petrographic evidence for primary hagendorfite in an unusual assemblage of phosphate minerals, Kibingo granitic pegmatite, Rwanda. Canadian Mineralogist, 42, 697–704.

Hatert, F., Fransolet, A.-M., and Maresch, W.V. (2006) The stability of primary alluaudites in granitic pegmatites: an experimental investigation of the $Na_2(Mn_{1-x}Fe_x^{2+})_2Fe^{3+}(PO_4)_3$ solid solution. Contributions to Mineralogy and Petrology, 152, 399–419.

Hatert, F., Ottolini, L., and Schmid-Beurmann, P. (2011) Experimental investigation of the alluaudite + triphylite assemblage, and development of the Na-in-triphylite geothermometer: Applications to natural pegmatite phosphates. Contributions to Mineralogy and Petrology, 161, 531–546.

Le Page, Y. and Donnay, G. (1977) The crystal structure of the new mineral maricíte, NaFePO4. Canadian Mineralogist, 15, 518–521.

Losey, A., Rakovan, J., Hughes, J.M., Francis, C.A., and Dyar, M.D. (2004) Structural variations in the lithiophilite-triphylite series and other olivine-group structures. Canadian Mineralogist, 42, 1105–1115.

Mandarino, J.A. (1981) The Gladstone-Dale relationship: Part IV. The compatibility concept and its application. Canadian Mineralogist, 19, 441–450.

Moore, P.B. (1972) Natrophilite, NaMnPO4, has ordered cations. American Mineralogist, 57, 1333–1344.

Oxford Diffraction (2007) CrysAlis CCD and CrysAlis RED, version 1.71. Oxford Diffraction, Oxford, England.

Palache, C., Berman, H., and Frondel, C. (1951) The System of Mineralogy, 7th edition, Vol. II. Wiley, New York.

Quensel, P. (1957) The paragenesis of the Varuträsk pegmatite, including a review of its mineral assemblage. Arkiv för Mineralogi och Geologi, 2(2), 9–125.

Roda, E., Fontan, F., Pesquera, A., and Velasco, F. (1996) The phosphate mineral association of the granitic pegmatites of the Fregeneda area (Salamanca, Spain). Mineralogical Magazine, 60, 767–778.

Sheldrick, G.M. (1990) SHELXTL, a crystallographic computing package, revision 4.1. Siemens Analytical X-Ray Instruments, Inc., Madison, Wisconsin.

——— (2008) A short history of SHELX. Acta Crystallographica, A64, 112–122.

Sturman, B.D., Mandarino, J.A., and Corlett, M.I. (1977) Maricíte, a sodium iron phosphate from the Big Fish River area, Yukon Territory, Canada. Canadian Mineralogist, 15, 396–398.

Vignola, P., Diella, V., Oppizzi, P., Tiepolo, M., and Weiss, S. (2008a) Phosphate assemblages from the Brissago granitic pegmatite, western Southern Alps, Switzerland. Canadian Mineralogist, 46, 635–650.

Vignola, P., Guastoni, A., and Diella, V. (2008b) Nb Ta Sn oxides association from the Malpensata granitic pegmatite, central Southern Alps (Lecco province, Italy): Magmatic differentiation, crystallization mechanism and geochemical inference. Geophysical Research Abstracts, EGU2008-A-03866.

Vignola, P., Hatert, F., Fransolet, A.-M., and Diella, V. (2010) The Na-rich phosphate minerals from Malpensata granitic pegmatite, Piona, Lecco province, Italy. Acta Mineralogica Petrographica, abstract series, 6, 609.

Vignola, P., Fransolet, A.-M., Diella, V., and Ferrari, E.S. (2011a) Complex mechanisms of alteration in a graftonite + sarcopside + triphylite association from the Luna pegmatite, Piona, Lecco province, Italy. Canadian Mineralogist, 49, 765–776.

Vignola, P., Hatert, F., Fransolet, A.-M., Medenbach, O., Diella, V, and Andò, S. (2011b) Karenwebberite, IMA 2011-015. CNMNC Newsletter No. 10, October 2011, page 2551; Mineralogical Magazine, 75, 2549–2561.

Wilson, A.J.C. (1992) International Tables for X-ray Crystallography, Vol. C, 883 p. Kluwer Academic Press, London.

```
data_nafepo1

_audit_creation_method          SHELXL-97
_chemical_name_systematic
;
 ?
;
_chemical_name_common           ?
_chemical_melting_point         ?
_chemical_formula_moiety        ?
_chemical_formula_sum
 'Fe0.75 Mn0.25 Na O4 P'
_chemical_formula_weight        173.58

loop_
 _atom_type_symbol
 _atom_type_description
 _atom_type_scat_dispersion_real
 _atom_type_scat_dispersion_imag
 _atom_type_scat_source
 'O'   'O'    0.0106    0.0060
 'International Tables Vol C Tables 4.2.6.8 and 6.1.1.4'
 'Na'  'Na'   0.0362    0.0249
 'International Tables Vol C Tables 4.2.6.8 and 6.1.1.4'
 'P'   'P'    0.1023    0.0942
 'International Tables Vol C Tables 4.2.6.8 and 6.1.1.4'
 'Fe'  'Fe'   0.3463    0.8444
 'International Tables Vol C Tables 4.2.6.8 and 6.1.1.4'
 'Mn'  'Mn'   0.3368    0.7283
 'International Tables Vol C Tables 4.2.6.8 and 6.1.1.4'

_symmetry_cell_setting              ?
_symmetry_space_group_name_H-M      ?

loop_
 _symmetry_equiv_pos_as_xyz
 'x, y, z'
 'x+1/2, -y+1/2, -z'
 '-x, -y, z+1/2'
 '-x+1/2, y+1/2, -z+1/2'
 '-x, -y, -z'
 '-x-1/2, y-1/2, z'
 'x, y, -z-1/2'
 'x-1/2, -y-1/2, z-1/2'

_cell_length_a                  4.8820(10)
_cell_length_b                  10.387(2)
_cell_length_c                  6.0910(12)
_cell_angle_alpha               90.00
_cell_angle_beta                90.00
_cell_angle_gamma               90.00
_cell_volume                    308.87(11)
_cell_formula_units_Z           4
_cell_measurement_temperature   293(2)
```

```
_cell_measurement_reflns_used        ?
_cell_measurement_theta_min          ?
_cell_measurement_theta_max          ?

_exptl_crystal_description           ?
_exptl_crystal_colour                ?
_exptl_crystal_size_max              ?
_exptl_crystal_size_mid              ?
_exptl_crystal_size_min              ?
_exptl_crystal_density_meas          ?
_exptl_crystal_density_diffrn        3.733
_exptl_crystal_density_method        'not measured'
_exptl_crystal_F_000                 335
_exptl_absorpt_coefficient_mu        5.217
_exptl_absorpt_correction_type       ?
_exptl_absorpt_correction_T_min      ?
_exptl_absorpt_correction_T_max      ?
_exptl_absorpt_process_details       ?

_exptl_special_details
;
 ?
;

_diffrn_ambient_temperature          293(2)
_diffrn_radiation_wavelength         0.71073
_diffrn_radiation_type               MoK\a
_diffrn_radiation_source             'fine-focus sealed tube'
_diffrn_radiation_monochromator      graphite
_diffrn_measurement_device_type      ?
_diffrn_measurement_method           ?
_diffrn_detector_area_resol_mean     ?
_diffrn_standards_number             ?
_diffrn_standards_interval_count     ?
_diffrn_standards_interval_time      ?
_diffrn_standards_decay_%            ?
_diffrn_reflns_number                861
_diffrn_reflns_av_R_equivalents      0.0390
_diffrn_reflns_av_sigmaI/netI        0.0472
_diffrn_reflns_limit_h_min           -6
_diffrn_reflns_limit_h_max           4
_diffrn_reflns_limit_k_min           -9
_diffrn_reflns_limit_k_max           13
_diffrn_reflns_limit_l_min           -8
_diffrn_reflns_limit_l_max           5
_diffrn_reflns_theta_min             3.92
_diffrn_reflns_theta_max             29.08
_reflns_number_total                 397
_reflns_number_gt                    375
_reflns_threshold_expression         >2sigma(I)

_computing_data_collection           ?
_computing_cell_refinement           ?
_computing_data_reduction            ?
_computing_structure_solution        'SHELXS-97 (Sheldrick, 1990)'
```

```
_computing_structure_refinement    'SHELXL-97 (Sheldrick, 1997)'
_computing_molecular_graphics       ?
_computing_publication_material     ?

_refine_special_details
;
 Refinement of F^2^ against ALL reflections.  The weighted R-factor wR and
 goodness of fit S are based on F^2^, conventional R-factors R are based
 on F, with F set to zero for negative F^2^. The threshold expression of
 F^2^ > 2sigma(F^2^) is used only for calculating R-factors(gt) etc. and is
 not relevant to the choice of reflections for refinement.  R-factors based
 on F^2^ are statistically about twice as large as those based on F, and R-
 factors based on ALL data will be even larger.
;

_refine_ls_structure_factor_coef  Fsqd
_refine_ls_matrix_type            full
_refine_ls_weighting_scheme       calc
_refine_ls_weighting_details
 'calc w=1/[\s^2^(Fo^2^)+(0.0800P)^2^+8.9000P] where P=(Fo^2^+2Fc^2^)/3'
_atom_sites_solution_primary      direct
_atom_sites_solution_secondary    difmap
_atom_sites_solution_hydrogens    geom
_refine_ls_hydrogen_treatment     mixed
_refine_ls_extinction_method      none
_refine_ls_extinction_coef        ?
_refine_ls_number_reflns          397
_refine_ls_number_parameters      43
_refine_ls_number_restraints      1
_refine_ls_R_factor_all           0.0835
_refine_ls_R_factor_gt            0.0785
_refine_ls_wR_factor_ref          0.2055
_refine_ls_wR_factor_gt           0.2023
_refine_ls_goodness_of_fit_ref    1.269
_refine_ls_restrained_S_all       1.267
_refine_ls_shift/su_max           0.001
_refine_ls_shift/su_mean          0.000

loop_
 _atom_site_label
 _atom_site_type_symbol
 _atom_site_fract_x
 _atom_site_fract_y
 _atom_site_fract_z
 _atom_site_U_iso_or_equiv
 _atom_site_adp_type
 _atom_site_occupancy
 _atom_site_symmetry_multiplicity
 _atom_site_calc_flag
 _atom_site_refinement_flags
 _atom_site_disorder_assembly
 _atom_site_disorder_group
Fe2 Fe 0.9862(4) 0.2827(2) 0.2500 0.0103(7) Uani 0.67(8) 2 d SP . .
Mn2 Mn 0.9862(4) 0.2827(2) 0.2500 0.0103(7) Uani 0.33(8) 2 d SP . .
P P 0.4334(8) 0.1034(4) 0.2500 0.0122(9) Uani 1 2 d S . .
```

```
Na1 Na 0.0000 0.0000 0.0000 0.018(3) Uani 0.68(3) 2 d SP . .
O1 O 0.744(2) 0.1113(11) 0.2500 0.019(2) Uani 1 2 d S . .
O2 O 0.166(3) 0.4648(9) 0.2500 0.020(2) Uani 1 2 d S . .
O3 O 0.3030(16) 0.1737(7) 0.0515(11) 0.0186(17) Uani 1 1 d . . .

loop_
 _atom_site_aniso_label
 _atom_site_aniso_U_11
 _atom_site_aniso_U_22
 _atom_site_aniso_U_33
 _atom_site_aniso_U_23
 _atom_site_aniso_U_13
 _atom_site_aniso_U_12
Fe2 0.0165(11) 0.0096(11) 0.0050(10) 0.000 0.000 -0.0008(7)
Mn2 0.0165(11) 0.0096(11) 0.0050(10) 0.000 0.000 -0.0008(7)
P 0.0168(18) 0.0127(17) 0.0071(16) 0.000 0.000 0.0017(14)
Na1 0.008(4) 0.025(5) 0.021(5) -0.003(4) -0.007(3) 0.002(3)
O1 0.019(5) 0.024(6) 0.015(5) 0.000 0.000 0.006(5)
O2 0.037(7) 0.010(5) 0.013(5) 0.000 0.000 -0.011(5)
O3 0.026(4) 0.025(4) 0.005(3) 0.008(3) 0.000(3) 0.006(3)

_geom_special_details
;
 All esds (except the esd in the dihedral angle between two l.s. planes)
 are estimated using the full covariance matrix.  The cell esds are taken
 into account individually in the estimation of esds in distances, angles
 and torsion angles; correlations between esds in cell parameters are only
 used when they are defined by crystal symmetry.  An approximate (isotropic)
 treatment of cell esds is used for estimating esds involving l.s. planes.
;

loop_
 _geom_bond_atom_site_label_1
 _geom_bond_atom_site_label_2
 _geom_bond_distance
 _geom_bond_site_symmetry_2
 _geom_bond_publ_flag
Fe2 O3 2.092(7) 2 ?
Fe2 O3 2.092(7) 8_666 ?
Fe2 O2 2.085(10) 1_655 ?
Fe2 O1 2.138(12) . ?
Fe2 O3 2.266(8) 7_656 ?
Fe2 O3 2.266(8) 1_655 ?
Fe2 Na1 3.3089(19) 1_655 ?
Fe2 Na1 3.3089(19) 3_655 ?
P O2 1.519(11) 6_655 ?
P O1 1.518(12) . ?
P O3 1.550(7) 7_556 ?
P O3 1.550(7) . ?
P Na1 2.819(3) . ?
P Na1 2.819(3) 3 ?
P Mn2 2.870(4) 1_455 ?
P Na1 3.335(3) 3_655 ?
P Na1 3.335(3) 1_655 ?
Na1 O2 2.261(9) 6_655 ?
```

```
Na1 O2 2.261(9) 2_455 ?
Na1 O1 2.284(8) 1_455 ?
Na1 O1 2.284(8) 5_655 ?
Na1 O3 2.354(8) . ?
Na1 O3 2.354(8) 5 ?
Na1 P 2.819(3) 5 ?
Na1 Na1 3.0455(6) 3 ?
Na1 Na1 3.0455(6) 3_554 ?
Na1 Mn2 3.3089(19) 5_655 ?
Na1 Fe2 3.3089(19) 5_655 ?
O1 Na1 2.284(8) 3_655 ?
O1 Na1 2.284(8) 1_655 ?
O2 P 1.519(11) 6_665 ?
O2 Fe2 2.085(10) 1_455 ?
O2 Mn2 2.085(10) 1_455 ?
O2 Na1 2.261(9) 4 ?
O2 Na1 2.261(9) 2 ?
O3 Mn2 2.092(7) 2_455 ?
O3 Fe2 2.092(7) 2_455 ?
O3 Mn2 2.266(8) 1_455 ?
O3 Fe2 2.266(8) 1_455 ?

loop_
 _geom_angle_atom_site_label_1
 _geom_angle_atom_site_label_2
 _geom_angle_atom_site_label_3
 _geom_angle
 _geom_angle_site_symmetry_1
 _geom_angle_site_symmetry_3
 _geom_angle_publ_flag
O3 Fe2 O3 122.8(4) 2 8_666 ?
O3 Fe2 O2 89.1(3) 2 1_655 ?
O3 Fe2 O2 89.1(3) 8_666 1_655 ?
O3 Fe2 O1 86.8(3) 2 . ?
O3 Fe2 O1 86.8(3) 8_666 . ?
O2 Fe2 O1 171.3(5) 1_655 . ?
O3 Fe2 O3 150.2(3) 2 7_656 ?
O3 Fe2 O3 86.07(17) 8_666 7_656 ?
O2 Fe2 O3 99.5(4) 1_655 7_656 ?
O1 Fe2 O3 87.8(3) . 7_656 ?
O3 Fe2 O3 86.07(17) 2 1_655 ?
O3 Fe2 O3 150.2(3) 8_666 1_655 ?
O2 Fe2 O3 99.5(4) 1_655 1_655 ?
O1 Fe2 O3 87.8(3) . 1_655 ?
O3 Fe2 O3 64.5(3) 7_656 1_655 ?
O3 Fe2 Na1 78.3(2) 2 1_655 ?
O3 Fe2 Na1 127.2(2) 8_666 1_655 ?
O2 Fe2 Na1 142.8(2) 1_655 1_655 ?
O1 Fe2 Na1 43.3(2) . 1_655 ?
O3 Fe2 Na1 77.77(18) 7_656 1_655 ?
O3 Fe2 Na1 45.3(2) 1_655 1_655 ?
O3 Fe2 Na1 127.2(2) 2 3_655 ?
O3 Fe2 Na1 78.3(2) 8_666 3_655 ?
O2 Fe2 Na1 142.8(2) 1_655 3_655 ?
O1 Fe2 Na1 43.3(2) . 3_655 ?
```

```
O3 Fe2 Na1 45.3(2) 7_656 3_655 ?
O3 Fe2 Na1 77.77(18) 1_655 3_655 ?
Na1 Fe2 Na1 54.80(4) 1_655 3_655 ?
O2 P O1 111.7(7) 6_655 . ?
O2 P O3 108.4(4) 6_655 7_556 ?
O1 P O3 112.6(4) . 7_556 ?
O2 P O3 108.4(4) 6_655 . ?
O1 P O3 112.6(4) . . ?
O3 P O3 102.6(6) 7_556 . ?
O2 P Na1 53.1(3) 6_655 . ?
O1 P Na1 140.4(3) . . ?
O3 P Na1 107.0(3) 7_556 . ?
O3 P Na1 56.6(3) . . ?
O2 P Na1 53.1(3) 6_655 3 ?
O1 P Na1 140.4(3) . 3 ?
O3 P Na1 56.6(3) 7_556 3 ?
O3 P Na1 107.0(3) . 3 ?
Na1 P Na1 65.38(9) . 3 ?
O2 P Mn2 111.8(5) 6_655 1_455 ?
O1 P Mn2 136.4(5) . 1_455 ?
O3 P Mn2 51.8(3) 7_556 1_455 ?
O3 P Mn2 51.8(3) . 1_455 ?
Na1 P Mn2 71.12(9) . 1_455 ?
Na1 P Mn2 71.12(9) 3 1_455 ?
O2 P Na1 87.7(4) 6_655 3_655 ?
O1 P Na1 35.8(3) . 3_655 ?
O3 P Na1 97.8(3) 7_556 3_655 ?
O3 P Na1 148.1(3) . 3_655 ?
Na1 P Na1 138.28(13) . 3_655 ?
Na1 P Na1 104.67(7) 3 3_655 ?
Mn2 P Na1 147.13(8) 1_455 3_655 ?
O2 P Na1 87.7(4) 6_655 1_655 ?
O1 P Na1 35.8(3) . 1_655 ?
O3 P Na1 148.1(3) 7_556 1_655 ?
O3 P Na1 97.8(3) . 1_655 ?
Na1 P Na1 104.67(7) . 1_655 ?
Na1 P Na1 138.28(13) 3 1_655 ?
Mn2 P Na1 147.13(8) 1_455 1_655 ?
Na1 P Na1 54.33(6) 3_655 1_655 ?
O2 Na1 O2 180.0(5) 6_655 2_455 ?
O2 Na1 O1 91.6(3) 6_655 1_455 ?
O2 Na1 O1 88.4(3) 2_455 1_455 ?
O2 Na1 O1 88.4(3) 6_655 5_655 ?
O2 Na1 O1 91.6(3) 2_455 5_655 ?
O1 Na1 O1 180.0(6) 1_455 5_655 ?
O2 Na1 O3 65.2(3) 6_655 . ?
O2 Na1 O3 114.8(3) 2_455 . ?
O1 Na1 O3 82.4(3) 1_455 . ?
O1 Na1 O3 97.6(3) 5_655 . ?
O2 Na1 O3 114.8(3) 6_655 5 ?
O2 Na1 O3 65.2(3) 2_455 5 ?
O1 Na1 O3 97.6(3) 1_455 5 ?
O1 Na1 O3 82.4(3) 5_655 5 ?
O3 Na1 O3 180.0(2) . 5 ?
O2 Na1 P 32.5(3) 6_655 . ?
```

O2 Na1 P 147.5(3) 2_455 . ?
O1 Na1 P 81.8(3) 1_455 . ?
O1 Na1 P 98.2(3) 5_655 . ?
O3 Na1 P 33.34(17) . . ?
O3 Na1 P 146.66(17) 5 . ?
O2 Na1 P 147.5(3) 6_655 5 ?
O2 Na1 P 32.5(3) 2_455 5 ?
O1 Na1 P 98.2(3) 1_455 5 ?
O1 Na1 P 81.8(3) 5_655 5 ?
O3 Na1 P 146.66(17) . 5 ?
O3 Na1 P 33.34(17) 5 5 ?
P Na1 P 180.0 . 5 ?
O2 Na1 Na1 47.7(2) 6_655 3 ?
O2 Na1 Na1 132.3(2) 2_455 3 ?
O1 Na1 Na1 48.20(18) 1_455 3 ?
O1 Na1 Na1 131.80(18) 5_655 3 ?
O3 Na1 Na1 82.34(16) . 3 ?
O3 Na1 Na1 97.66(16) 5 3 ?
P Na1 Na1 57.31(4) . 3 ?
P Na1 Na1 122.69(4) 5 3 ?
O2 Na1 Na1 132.3(2) 6_655 3_554 ?
O2 Na1 Na1 47.7(2) 2_455 3_554 ?
O1 Na1 Na1 131.80(18) 1_455 3_554 ?
O1 Na1 Na1 48.20(18) 5_655 3_554 ?
O3 Na1 Na1 97.66(16) . 3_554 ?
O3 Na1 Na1 82.34(16) 5 3_554 ?
P Na1 Na1 122.69(4) . 3_554 ?
P Na1 Na1 57.31(4) 5 3_554 ?
Na1 Na1 Na1 180.0 3 3_554 ?
O2 Na1 Mn2 98.7(2) 6_655 5_655 ?
O2 Na1 Mn2 81.3(2) 2_455 5_655 ?
O1 Na1 Mn2 140.1(3) 1_455 5_655 ?
O1 Na1 Mn2 39.9(3) 5_655 5_655 ?
O3 Na1 Mn2 136.79(18) . 5_655 ?
O3 Na1 Mn2 43.21(18) 5 5_655 ?
P Na1 Mn2 124.84(8) . 5_655 ?
P Na1 Mn2 55.16(8) 5 5_655 ?
Na1 Na1 Mn2 117.400(18) 3 5_655 ?
Na1 Na1 Mn2 62.600(18) 3_554 5_655 ?
O2 Na1 Fe2 98.7(2) 6_655 5_655 ?
O2 Na1 Fe2 81.3(2) 2_455 5_655 ?
O1 Na1 Fe2 140.1(3) 1_455 5_655 ?
O1 Na1 Fe2 39.9(3) 5_655 5_655 ?
O3 Na1 Fe2 136.79(18) . 5_655 ?
O3 Na1 Fe2 43.21(18) 5 5_655 ?
P Na1 Fe2 124.84(8) . 5_655 ?
P Na1 Fe2 55.16(8) 5 5_655 ?
Na1 Na1 Fe2 117.400(18) 3 5_655 ?
Na1 Na1 Fe2 62.600(18) 3_554 5_655 ?
Mn2 Na1 Fe2 0.00(8) 5_655 5_655 ?
P O1 Fe2 126.7(7) . . ?
P O1 Na1 121.3(5) . 3_655 ?
Fe2 O1 Na1 96.8(4) . 3_655 ?
P O1 Na1 121.3(5) . 1_655 ?
Fe2 O1 Na1 96.8(4) . 1_655 ?

```
Na1 O1 Na1 83.6(4) 3_655 1_655 ?
P O2 Fe2 136.4(8) 6_665 1_455 ?
P O2 Mn2 136.4(8) 6_665 1_455 ?
Fe2 O2 Mn2 0.00(10) 1_455 1_455 ?
P O2 Na1 94.4(4) 6_665 4 ?
Fe2 O2 Na1 116.8(4) 1_455 4 ?
Mn2 O2 Na1 116.8(4) 1_455 4 ?
P O2 Na1 94.4(4) 6_665 2 ?
Fe2 O2 Na1 116.8(4) 1_455 2 ?
Mn2 O2 Na1 116.8(4) 1_455 2 ?
Na1 O2 Na1 84.7(4) 4 2 ?
P O3 Mn2 127.7(5) . 2_455 ?
P O3 Fe2 127.7(5) . 2_455 ?
Mn2 O3 Fe2 0.00(11) 2_455 2_455 ?
P O3 Mn2 95.7(3) . 1_455 ?
Mn2 O3 Mn2 130.7(3) 2_455 1_455 ?
Fe2 O3 Mn2 130.7(3) 2_455 1_455 ?
P O3 Fe2 95.7(3) . 1_455 ?
Mn2 O3 Fe2 130.7(3) 2_455 1_455 ?
Fe2 O3 Fe2 130.7(3) 2_455 1_455 ?
Mn2 O3 Fe2 0.00(7) 1_455 1_455 ?
P O3 Na1 90.0(3) . . ?
Mn2 O3 Na1 108.5(3) 2_455 . ?
Fe2 O3 Na1 108.5(3) 2_455 . ?
Mn2 O3 Na1 91.4(3) 1_455 . ?
Fe2 O3 Na1 91.4(3) 1_455 . ?

_diffrn_measured_fraction_theta_max     0.876
_diffrn_reflns_theta_full               29.08
_diffrn_measured_fraction_theta_full    0.876
_refine_diff_density_max      1.120
_refine_diff_density_min     -2.204
_refine_diff_density_rms      0.311
```